Table I. Kinetic Parameters and Estimated Transmission Coefficients in Some Simple Electron-Transfer Reactions

oxidant	λ_{max},[a] nm (ϵ, M^{-1} cm^{-1})	k,[b] M^{-1} s^{-1} Co(sep)$^{2+}$	k,[b] M^{-1} s^{-1} Ru(NH$_3$)$_6$$^{2+}$	$R(X)_{obsd}$[c]	$\sim\kappa_{el}$[d]	AE,[e] eV
$Co(NH_3)_5Cl^{2+}$	525 (80)	58 ± 4	260 ± 20	0.22	0.03	
cis-$Co(en)_2(cha)Cl^{2+}$	525 (83)	0.82 ± 0.06	45 ± 4	0.018	0.0012	<<−1
cis-$Co(en)_2(C_6H_5NH_2)Cl^{2+}$	525 (83)	3.3 ± 0.3	56 ± 5	0.06	0.004	−1.13
cis-$Co(en)_2(p\text{-}NO_2C_6H_4NH_2)Cl^{2+}$	520 (85)	92 ± 6	81 ± 5	1.1	0.1	>0
$Co(NH_3)_5(C_6H_5NH_2)^{3+}$	480 (66)	0.60 ± 0.05	0.11 ± 0.01	5.5	0.1	
$Co(NH_3)_5(p\text{-}NO_2C_6H_4NH_2)^{3+}$	483 (59)	2.1 ± 0.2	0.14 ± 0.01	15	0.3	

[a] Lowest energy absorption maximum, $\sim(^1A_1 \rightarrow {}^1T_1)$. [b] Mean and mean deviation of four to six determinations (25 °C, 0.20 M $NaCF_3SO_3$). [c] $R(X)_{obsd} = k^{Co}/k^{Ru}$). [d] $\kappa_{el} = R(X)_{obsd}/R(X)_{ad}$; see text and ref 17. [e] Electron affinity energies for the reaction Am + $e^- \rightarrow Am^-$ based on ref 13.

Co(sep)$^{2+}$ to Ru(NH$_3$)$_6$$^{2+}$ reductions as a measure of the nonadiabaticity of the Co(III)–Co(sep)$^{2+}$ reactions since, on the basis of the Marcus square root relation,[14] first-order Franck–Condon contributions of the oxidant (X) cancel in the ratio; i.e.

$$R(X) = k^{Co}(X)/k^{Ru}(X) = [k_{exch}{}^{Co}K(Co,Ru)/k_{exch}{}^{Ru}]^{1/2}[f^{Co}(X)/f^{Ru}(X)]^{1/2}$$

where $k_{exch}{}^{Co}$ and $k_{exch}{}^{Ru}$ are the self-exchange rate constants for Co(sep)$^{3+,2+}$ and Ru(NH$_3$)$_6$$^{3+,2+}$ respectively, K(Co,Ru) is the Co(sep)$^{2+}$–Ru(NH$_3$)$_6$$^{3+}$ equilibrium constant, and log $f^i(X) = 2 \log [K(X,i)]/4 \log (k_{exch}{}^{X}k_{exch}{}^{i}/A^2)$, with A = preexponential component of the rate constant expression[8c] and i = Co(sep)$^{2+}$ or Ru(NH$_3$)$_6$$^{2+}$. Even for adiabatic reactions R(X) will vary from oxidant to oxidant through the second-order $f^i(X)$ terms; this variation is far more sensitive to differences in K(X,i) than in k^X. To compensate for this, a small correction has been made for the oxidant contributions to observed values of R(X). For Co(en)$_3$$^{3+}$ and Co(NH$_3$)$_6$$^{3+}$ the adiabatic value of $R(X)_{ad} \simeq 42$,[15] and this value has been used as a reference value for $\kappa_{el} \simeq R(X)_{obsd}/R(X)_{ad}$ of the Co(NH$_3$)$_5$Am^{3+} oxidants in Table I. Substitution of an amine (or NH$_3$) by Cl$^-$ renders the complex slightly more oxidizing,[16] and for the chloropentaammine complexes we have used $R(X)_{ad}$ = 15.[17]

There is a clear and dramatic increase in efficiency of Co(sep)$^{2+}$ reductions of Co(en)$_2$(Am)Cl^{2+} complexes when Am is varied from a saturated amine (cyclohexylamine = cha) to *p*-nitroaniline, with $R(X)_{obsd}$ (or κ_{el}) increasing by about 10^2. The very different rates of reduction, as well as the smaller than adiabatic rate ratios, found for reductions of *cis*-Co(en)$_2$(*p*-NO$_2$C$_6$H$_4$NH$_2$)Cl^{2+} and Co(NH$_3$)$_5$(*p*-NO$_2$C$_6$H$_4$NH$_2$)$^{3+}$ rule out intervention of direct reduction of the ligand.

We have elsewhere noted[3c,d,12,16b] for related reactions that, in the absence of CT perturbations, the more similar the electronic structures of reactants and products, the more nearly adiabatic are the experimentally observed electron-transfer rates. Thus, Co(sep)$^{2+}$ reductions of Co^{III}(Am)$_6$ complexes tend to approach the adiabatic limit while the *cis*-Co(en)$_2$(cha)Cl^{2+}–Co(sep)$^{2+}$ reaction is the least adiabatic reaction of this class that we have found.[16b] This behavior can be mostly ascribed to an increase in the effective value of ψ^{III}, and therefore in J, as the oxidized reactant and product species become more similar in electronic structure (one expects a related, but probably smaller, contribution from ψ^{II}). For J sufficiently large, $\kappa_{el} \rightarrow 1$, and CT perturbations no longer contribute much to the reactivity patterns.[3d,16d] Thus, we find only a small difference in the electron-transfer behavior of Co(NH$_3$)$_5$(C$_6$H$_5$NH$_2$)$^{3+}$ and Co(NH$_3$)$_5$(*p*-NO$_2$C$_6$H$_4$NH$_2$)$^{3+}$, in contrast to relatively large differences in the electron-transfer behavior of *cis*-Co(en)$_2$(C$_6$H$_5$NH$_2$)Cl^{2+} and *cis*-Co(en)$_2$(*p*-NO$_2$C$_6$H$_4$NH$_2$)Cl^{2+} (see Table I). We can now add MLCT to LMCT perturbations as the kinds of environmental factors that enhance electronic coupling between spatially separated donors and acceptors.

We find that the concept of electron exchange coupling of reactant and product potential energy surfaces is very useful in the design of experiments that explore the nonadiabatic behavior of simple electron-transfer reactions and also in the interpretation of this behavior. The exchange[4] and tunneling[2d,e] formulations provide somewhat different approaches to the description of the electronic matrix element. Insofar as each of these approaches provides a reasonable approximation to the physical situation, each will provide a means for interpreting the variations in adiabaticity of electron-transfer reactions. At a very primitive, intuitive level, the tunneling formalism focuses on the properties of the donor while the exchange formalism gives equal weight to donor and acceptor. Thus, the observation that both LMCT and MLCT perturbations can alter the extent of donor–acceptor coupling seems superficially more readily accommodated in the context of the exchange formalism. Nevertheless, the induced dipole moments of the LMCT and MLCT perturbations that we have examined do have a similar directional sense with respect to the donor–acceptor axis, and it is probably possible to adjust the tunneling parameters to accommodate these observations.

Registry No. Co(sep)$^{2+}$, 63218-22-4; Ru(NH$_3$)$_6$$^{2+}$, 19052-44-9; *cis*-Co(en)$_2$(cha)Cl^{2+}, 28121-20-2; *cis*-Co(en)$_2$(C$_6$H$_5$NH$_2$)Cl^{2+}, 46753-03-1; *cis*-Co(en)$_2$(*p*-NO$_2$C$_6$H$_4$NH$_2$)Cl^{2+}, 91312-06-0; Co(NH$_3$)$_5$Cl^{2+}, 14970-14-0; Co(NH$_3$)$_5$(PhNH$_2$)$^{3+}$, 91312-07-1; Co(NH$_3$)$_5$(*p*-NO$_2$C$_6$H$_4$NH$_2$)$^{3+}$, 91312-08-2.

Department of Chemistry
Wayne State University
Detroit, Michigan 48202

T. Ramasami
John F. Endicott*

Received December 19, 1983

---

(14) Marcus, R. A.: (a) *Annu. Rev. Phys. Chem.* **1964**, *15*, 155; (b) *Discuss. Faraday Soc.* **1960**, *29*, 21.

(15) Endicott, J. F.; Brubaker, G. R.; Ramasami, T.; Kumar, K.; Dwarakanath, K.; Cassel, J. *Inorg. Chem.* **1983**, *22*, 3754.

(16) (a) Rillema, D. P.; Endicott, J. F.; Papaconstantinou, E. *Inorg. Chem.* **1971**, *10*, 1739. (b) Ramasami, T.; Endicott, J. F., to be submitted for publication.

(17) This value is based on the ratio of rates of reaction of Co(NH$_3$)$_5$Cl^{2+} with Cr(bpy)$_3$$^{2+}$ and Ru(NH$_3$)$_6$$^{2+}$ (Ramasami, T.; Endicott, J. F., unpublished results). The Cr(bpy)$_3$$^{3+,2+}$ couple has about the same reduction potential as the Co(sep)$^{3+,2+}$ couple, but the chromium couple should be relatively adiabatic.

X-ray Structure and Physical Properties of the Mixed-Valence Compound 1,12-Dimethyl[1.1]ferrocenophanium Triiodide

Sir:

The study of electron transfer in mixed-valence complexes leads to insight about electron transfer in oxidation–reduction, electrochemical, and biological processes.[1] Bridged ferrocenes

0020-1669/84/1323-2918$01.50/0

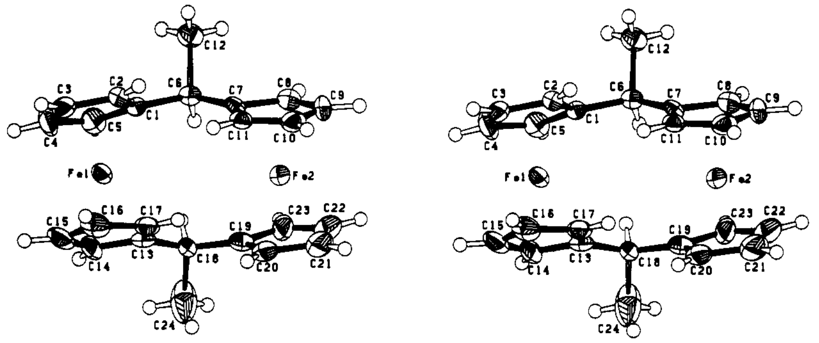

Figure 1. ORTEP stereoview of the 1,12-dimethyl[1.1]ferrocenophanium monocation (**1**) with 35% probability ellipsoids.

have proven to be good candidates for mixed-valence compounds due to their variability in structure and suitability for study with several physical techniques.[2] [1.1]Ferrocenophanes such as 1,12-dimethyl[1.1]ferrocenophane (the unoxidized form of **1**) are particularly attractive precursors for the formation of mixed-valence bridged ferrocenes. A study of the single-crystal X-ray structure and physical properties of the mixed-valence I_3^- salt of monocation **1** where one iron ion is oxidized was undertaken for three reasons. First, Hillman and Kvick[3] very recently reported that the Fe–Fe distance (3.636 (1) Å) in the analogous mixed-valence bis(fulvalene)diiron cation is 0.35 Å shorter than in the corresponding neutral Fe(II)–Fe(II) complex. The bis(fulvalene)diiron framework distorts so as to increase the direct Fe–Fe interaction in the mixed-valence cation. Does the same type of movement of iron ions and distortion occur in monocation **1** to increase the Fe–Fe interaction? Second, Bitterwolf and Ling[4] have shown that [1.1]ferrocenophanes react with acids to give H_2 and cationic (carbocations) forms of [1.1]ferrocenophanes. Very recently Mueller-Westerhoff et al.[5] reported the X-ray structure of the BF_4^- salt of the monocation of [1.1]-ferrocenophane (**2**), where a hydride ion has been removed from one of the bridging carbon atoms to give a carbenium cation. A comparison of the dimensions of the carbenium ion **2** with the mixed-valence Fe(III)–Fe(II) cation **1** would be interesting. Third, previous ^{57}Fe Mössbauer work[6] on the mixed-valence I_3^- salt of the monocation **1** suggested that in the solid state both the valence-localized and valence-delocalized forms of the monocation **1** are present. It was of interest to see whether these two forms differed in Fe–Fe distances. In the X-ray structure[7] of the neutral unoxidized form of **1**, there are, in fact, two different molecules in the asymmetric unit with different Fe–Fe distances [4.620 (2) and 4.595 (2) Å].

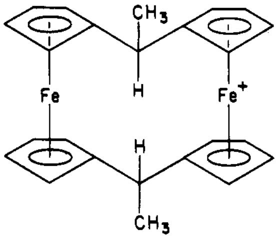

1

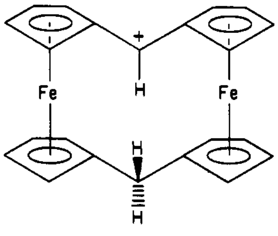

2

Single crystals of the mixed-valence I_3^- salt of **1** were prepared by the slow evaporation under argon of a CH_2Cl_2 solution of unoxidized **1** and a stoichiometric amount of I_2. The room-temperature single-crystal X-ray structure was determined by direct-method techniques.[8] There is only one monocation **1** in the asymmetric unit; the monocation assumes a syn conformation as illustrated in Figure 1. The two metallocene units in **1** are not equivalent. As found before for the mixed-valence diferrocenylselenium monocation ($I_3^-{\cdot}I_2{\cdot}{}^1/_2CH_2Cl_2$ salt),[9] the centroid-to-centroid distance [3.31 (2) Å] between the two rings associated with the atom labeled Fe1 (see Figure 1) indicates that this metallocene unit is in the Fe(II) oxidation state, whereas the centroid-to-centroid distance [3.39 (2) Å] associated with Fe2 indicates that this is the Fe(III) metallocene moiety.

This mixed-valence monocation is a class I ion as indicated by the absence of an IT electronic absorption band in the near-infrared region.

It is interesting that the Fe–Fe distance in the mixed-valence monocation **1** is 4.599 (2) Å, a value that is between the values for the two different Fe–Fe distances reported[7] for the unoxidized form of **1** (vide supra). Clearly, there is little movement of the two iron ions in this monocation, as was observed[3] in the bis(fulvalene)diiron monocation.

A comparison of the structure of the mixed-valence monocation **1** (Figure 1) with the structure reported[5] for the carbenium monocation **2** (BF_4^- salt) is interesting. There are two main differences. As can be seen in Figure 1, the two metallocene moieties in the mixed-valence Fe(III)–Fe(II) monocation of **1** are more twisted away from being side by side compared to their positioning in **2**. More importantly, the four distances between the two iron ions in mixed-valence monocation **1** and the bridging carbon atoms C6 and C18 are all about equal (3.3 Å). As indicated by bond angles, atoms C6 and C18 are sp^3 hybridized in **1**. On the other hand, the apparently positively charged carbon atom in **2** is noticeably drawn toward the center of the cation, lying approximately 0.20 Å below the intersection of the two adjacent cyclopentadienyl ring planes [$Fe{\cdots}C^+$ distances of 2.96 (2) and 3.01 (2) Å]. The "positive" carbon atom in **2** moves to interact with the two iron ions.

The last point to address is what is the origin of the valence-delocalized ^{57}Fe Mössbauer signal reported[6] previously for the I_3^- salt of the mixed-valence monocation **1**? The X-ray

---

(1) Brown, D. B., Ed. "Mixed-Valence Compounds, Theory and Applications in Chemistry, Physics, Geology, and Biology"; D. Reidel Publishing Co.: Boston, MA, 1979.

(2) Kramer, J. A.; Hendrickson, D. N. *Inorg. Chem.* **1980**, *19*, 3330–3337 and references therein.

(3) Hillman, M.; Kvick, A. *Organometallics* **1983**, *2*, 1780–1785.

(4) Bitterwolf, T. E.; Ling, A. C. *J. Organomet. Chem.* **1973**, *57*, C15.

(5) Mueller-Westerhoff, U. T.; Nazzal, A.; Prossdorf, W.; Mayerle, J. J.; Collins, R. L. *Angew. Chem., Int. Ed. Engl.* **1982**, *4*, 293–294.

(6) (a) Morrison, W. H., Jr.; Hendrickson, D. N. *Inorg. Chem.* **1975**, *14*, 2331–2346. (b) Morrison, W. H., Jr.; Hendrickson, D. N. *Chem. Phys. Lett.* **1973**, *22*, 119–123.

(7) (a) McKechnie, J. S.; Bersted, B.; Paul, I. C.; Watts, W. E. *J. Organomet. Chem.* **1967**, *8*, 29. (b) McKechnie, J. S.; Maier, C. A.; Bersted, B.; Paul, I. C. *J. Chem. Soc., Perkins Trans. 2* **1973**, *2*, 138.

(8) The crystal measured 0.14 mm × 0.22 mm × 0.28 mm, and μ was 49.37 cm^{-1} (Mo Kα). Crystallographic data: space group $P2_1/c$, a = 9.458 (2) Å, b = 19.794 (6) Å, c = 13.776 (3) Å, β = 108.23 (2)°, ρ_{calcd} = 2.182 g cm^{-3}, Z = 4, fw = 804.86. The intensities of 2672 unique, observed [$I > 2.58\sigma(I)$] reflections were determined. The final structural model involved anisotropic thermal parameters for all non-hydrogen atoms. This model refined to convergence with R = 0.053 and R_w = 0.045.

(9) Kramer, J. A.; Herbstein, F. H.; Hendrickson, D. N. *J. Am. Chem. Soc.* **1980**, *102*, 2293–2301.

structure only shows one monocation that is valence localized. Mössbauer spectra were collected in the range of 300–120 K for a microcrystalline sample of the I_3^- salt of **1** prepared from CH_2Cl_2 as was the crystal employed in the structure determination. No quadrupole-split doublet ($\Delta E_Q \simeq 1.85$ mm/s) that could be assigned to a Mössbauer-delocalized complex could be seen; only one Fe(III) doublet and one Fe(II) doublet could be seen. In the previous work,[6] the I_3^- salt of the mixed-valence monocation **1** was prepared from benzene with an *excess* of I_2, not from CH_2Cl_2 with a stoichiometric amount of I_2. Additional work that will be described in a later paper suggests that the valence-delocalized Mössbauer doublet reported[6] before comes from the I_3^- salt of the carbenium cation form of **1** that inadvertently precipitates from benzene.

Acknowledgment. We are grateful for funding from the National Institutes of Health (Grant HL13652).

Supplementary Material Available: Tables of positional parameters, thermal parameters, and structure factors (14 pages). Ordering information is given on any current masthead page.

School of Chemical Sciences
University of Illinois
Urbana, Illinois 61801

Michael F. Moore
Scott R. Wilson
David N. Hendrickson*

Department of Chemistry
University of Connecticut
Storrs, Connecticut 06268

Ulrich T. Mueller-Westerhoff

Received April 2, 1984

The Framework Chemistry of Zeolites: ^{27}Al MASNMR of Extralattice Tetrahedral Aluminum Species

Sir:

The chemical, physical, and catalytic properties of zeolites are greatly influenced by their framework and nonframework composition. The aluminum content of the zeolite framework can be modified by chemical and/or thermal treatments. Numerous procedures have been developed. Chemical treatments of zeolites with $SiCl_4$,[1] for example, result in high-silica forms. Perhaps the most widely used technique is hydrothermal treatment.[2] These procedures are believed to increase the framework Si/Al ratio by effecting a migration of framework aluminum into nonlattice positions and in some cases from the zeolite. The exact nature of the extralattice aluminum species, the mechanism of this dealumination, the remaining framework defect structure, and the mechanism by which it is cured are not known. We present here the results of a study in which the formation of a nonframework tetrahedral aluminum species upon dealumination by thermal treatment of ion-exchanged zeolite A is followed by ^{29}Si and ^{27}Al MASNMR.

Pluth and Smith have reported finding electron density in the center of the sodalite unit in the determination of the crystal structures of dehydrated Ca^{2+}- and Sr^{2+}-exchanged zeolite A.[3,4] They have assumed this to be partial occupancy by disordered AlO_4^* species. This electron density has been observed for Ca–X as well as most samples of zeolite A exchanged with divalent cations, but not the monovalent-exchanged samples.[4,5] Although Basler and Maiwald[6] have found ^{1}H NMR evidence for an aluminum species occluded during synthesis in the sodalite unit of zeolite Na–A dried at 90 °C, the absence of AlO_4^* in their structural solution of monovalent-exchanged zeolite A led Pluth and Smith to suggest that the aluminate species develops during ion exchange with divalent ions or during the subsequent dehydration.

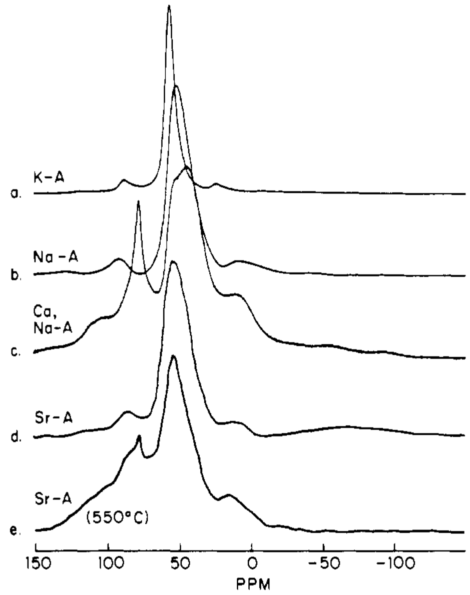

Figure 1. ^{27}Al MASNMR spectra of K–A, Na–A, Ca,Na–A, Sr–A, and Sr–A (550 °C).

We have also previously reported evidence from neutron powder diffraction studies for a 4-coordinate aluminum species in the center of the sodalite unit in H–Y zeolites treated with steam/NH_3 and $SiCl_4$.[7]

High-resolution magic angle spinning NMR (MASNMR) has recently been shown to be a very useful tool for zeolite characterization[8] of both the framework composition and extralattice species. Silicon-29 MASNMR is particularly useful for studying the change in the silicon–aluminum ordering in the zeolite framework upon treatment.[9] Aluminum-27 MASNMR has been used in the differentiation of the tetrahedral aluminum sites from the extralattice sites generated on steaming[10] and $SiCl_4$ treatment.[11] For both cases, 6-coordinate extralattice aluminum has been observed. In the unwashed $SiCl_4$-treated zeolites, a tetrahedral $AlCl_4^-$ species has also been identified. More recently, Engelhardt et al.[12] have used ^{27}Al MASNMR to study room-temperature dried

---

(1) Beyer, H. K.; Belenykaja, I. In "Catalysis by Zeolites"; Imelik, B., et al., Eds.; Elsevier: Amsterdam, 1980; pp 203–210.

(2) Scherzer, J. *J. Catal.* **1978**, *54*, 285 and references therein.

(3) Pluth, J. J.; Smith, J. V. *J. Am. Chem. Soc.* **1983**, *105*, 1192.

(4) Pluth, J. J.; Smith, J. V. *J. Am. Chem. Soc.* **1982**, *104*, 6977.

(5) Although the density for the corresponding oxygen atoms for a vacuum-dehydrated silver hydrogen zeolite A was not found, electron density at the center of the sodalite unit was reported and assigned as aluminum (Gellens, L. R.; Smith, J. V.; Pluth, J. J. *J. Am. Chem. Soc.* **1983**, *105*, 51).

(6) Basler, W. D.; Maiwald, W. *J. Phys. Chem.* **1979**, *83*, 2148. Basler, W. D.; Maiwald, W. In "Magnetic Resonance in Colloid and Interface Science"; Fraissaid, J. P., Resing, H. A., Eds.; Reidel: Boston, 1980; pp 437–442.

(7) Parise, J. B.; Corbin, D. R.; Abrams, L.; Cox, D. E. *Acta Crystallogr., Sect. C*, in press.

(8) Lippmaa, E.; Mägi, M.; Samoson, A.; Engelhardt, G.; Grimmer, A.-R. *J. Am. Chem. Soc.* **1980**, *102*, 4889. Melchior, M. T.; Vaughan, D. E. W.; Jarman, R. H.; Jacobson, A. J. *Nature (London)* **1982**, *298*, 455. Fyfe, C. A.; Thomas, J. M.; Klinowski, J.; Gobbi, G. C. *Angew. Chem., Int. Ed. Engl.* **1983**, *22*, 259–275.

(9) Vega, A. J. In "Intrazeolite Chemistry", Stucky, G. D., Dwyer, F. G., Eds.; American Chemical Society: Washington, D.C., 1983; pp 217–230.

(10) Maxwell, I. E.; von Erp, W. A.; Hays, G. R.; Couperus, T.; Huis, R.; Clague, A. D. H. *J. Chem. Soc., Chem. Commun.* **1982**, 523.

(11) Klinowski, J.; Thomas, J. M.; Fyfe, C. A.; Gobbi, G. C.; Hartman, J. S. *Inorg. Chem.* **1983**, *22*, 63.

(12) Engelhardt, G.; Fahlke, B.; Mägi, M.; Lippmaa, E. *Zeolites* **1983**, *3*, 292.

0020-1669/84/1323-2920$01.50/0